

1459
1460
1461
1462
1463
1464
1465
1466
1467
1468
1469
1470
1471
1472
1473
1474
1475
1476
1477
1478
1479
1480
1481
1482
1483
1484
1485
1486
1487
1488
1489
1490
1491
1492
1493
1494
1495
1496
1497
1498
1499
1500

Far-Infrared Hydrogen Lasers in the Peculiar Star MWC 349A

Vladimir Strel'nitski,* Michael R. Haas, Howard A. Smith,
Edwin F. Erickson, Sean W. J. Colgan, and David J. Hollenbach

Far-Infrared Hydrogen Lasers in the Peculiar Star MWC 349A

Vladimir Strel'nitski,* Michael R. Haas, Howard A. Smith, Edwin F. Erickson, Sean W. J. Colgan, David J. Hollenbach

Far-infrared hydrogen recombination lines H15 α (169.4 micrometers), H12 α (88.8 micrometers), and H10 α (52.5 micrometers) were detected in the peculiar luminous star MWC 349A from the Kuiper Airborne Observatory. Here it is shown that at least H15 α is strongly amplified, with the probable amplification factor being greater than or about equal to 10^3 and a brightness temperature that is greater than or about equal to 10^7 kelvin. The other two lines also show signs of amplification, although to a lesser degree. Beyond H10 α the amplification apparently vanishes. The newly detected amplified lines fall into the laser wavelength domain. These lasers, as well as the previously detected hydrogen masers, may originate in the photoionized circumstellar disk of MWC 349A and constrain the disk's physics and structure.

Soon after the invention of the maser and laser (microwave and light amplification by the stimulated emission of radiation, respectively), natural masers with amplifications A up to 10^{12} were discovered in interstellar and circumstellar gas clouds (1), first at centimeter wavelengths and later in the millimeter and submillimeter domains, down to wavelengths $\lambda \approx 0.45$ mm (450 μm) (2, 3). The search for natural masers (or, rather, lasers) at still shorter wavelengths is severely hampered by the opacity of our atmosphere. In fact, throughout most of the 300- to 20- μm region, ground-based observations are impossible.

Masers and lasers work on the same physical principle. In the laboratory, the distinction made between them is based on the technology used to create them, with the wavelength boundary lying roughly at several hundred micrometers (4). A natural dividing principle in astrophysics is the detection technology: the microwave ("wave detecting") technology used for masers and the optical ("quantum detecting") technology used for lasers. This boundary roughly coincides with that between laboratory masers and lasers and

also with the above-mentioned 300- μm observational barrier.

There is no reason to doubt the existence of astrophysical lasers. For example, calculations have predicted population inversions (5)—a necessary condition for amplification—and, in some cases, the possibility of high gains (6) in the optical and near-infrared hydrogen transitions in HII regions (which are hydrogen clouds ionized by the ultraviolet radiation of nearby hot stars). Yet there is a puzzling lack of observed astrophysical lasers. In 1979, Smith *et al.* (7) reported an abnormally bright line at $\lambda = 4.7$ μm in the spectrum of the Becklin-Neugebauer object in Orion. The line was identified as the hydrogen Pf β transition and, on the basis of an analysis of level populations, it was argued that it might be lasing. However, when this observation was repeated, the line was not as bright (8). Within the solar system, there is strong evidence for population inversions in the 10- μm CO₂ bands in the martian and venusian atmospheres (9). However, the predicted amplifications are very small ($A \leq 1.1$) and are not yet sufficient to discriminate observationally between lasing and spontaneous fluorescence. Besides, the energies involved are $\sim 10^{15}$ times smaller than the typical energies of the galactic masers. Thus, this local phenomenon is not the long-sought optical-infrared analog of the powerful, high-gain astrophysical masers.

Looking for an object that could help solve this 30-year puzzle of why astrophysi-

cal masers are observed and lasers are not, we chose MWC 349A. This luminous star, $\approx 30,000 L_{\odot}$ (10), is surrounded by a massive ionized envelope that has been detected in more than 20 hydrogen emission α lines—from the visual H2 α line (11) at 0.65 μm to the radio H92 α line (12) at 3 cm. (Hn α denotes the hydrogen transition between the levels with principal quantum numbers n and $n + 1$.) Several of the α lines in the millimeter domain were found to have a peculiar velocity structure: two intense, narrow spectral peaks superimposed on a broad component similar to that found for other transitions (13). The narrowness and the high intensity of the double-peaked component have been attributed to masing (13). The double-peaked component first appears at H36 α (2.2 mm) and is seen down to H21 α (0.45 mm)—the shortest wavelength submillimeter α line observable from the ground (2, 13–16). Yet the optical and near-infrared α lines show no sign of lasing (17). Thus, MWC 349A was a promising candidate for detecting the first high-gain astrophysical lasers in the far-infrared domain and for studying the transition from the apparently amplified long-wavelength lines to the apparently nonamplified short-wavelength lines. The latter could shed light on the puzzle of the lack of observed lasers in general.

We observed the H10 α line at 52.5 μm on 15 June 1994 and the H12 α and H15 α lines at 88.8 and 169.4 μm on 16 August 1995 with the 91-cm telescope of the Kuiper Airborne Observatory (KAO), using the facility's cryogenic grating spectrometer (18, 19). Spectral resolutions were ≈ 80 , 80, and 140 km s^{-1} , respectively, and the measured fluxes were $36 \pm 13 \times 10^{-20}$, $5.5 \pm 2.5 \times 10^{-20}$, and $8.1 \pm 1.9 \times 10^{-20} \text{ W cm}^{-2}$, respectively. The H12 α measurement is slightly above 2σ and is formally only an upper limit. The H10 α line is measured to nearly 3σ and is a probable detection (20). The H15 α line is more than 4σ and is clearly a solid detection (Fig. 1). The fact that all three lines are observed to fall within one-quarter channel of their expected wavelengths, which is well within our calibration uncertainty of ± 0.5 channels, increases confidence in these results. No other atomic or molecular features of any significant strength are expected in any of these bandpasses.

A convincing case for lasing in the newly detected lines can be made by comparing their fluxes with those at other wavelengths and using simple phenomenological arguments concerning the nature of the emission. The nonmasing parts of MWC 349A's envelope radiate spontaneous emission in the α lines, which is partially reabsorbed by the free electrons

V. Strel'nitski and H. A. Smith, Laboratory for Astrophysics, National Air and Space Museum, Smithsonian Institution, Washington, DC 20560, USA.

M. R. Haas, E. F. Erickson, D. J. Hollenbach, NASA Ames Research Center, Moffett Field, CA 94035–1000, USA. S. W. J. Colgan, NASA Ames Research Center, Moffett Field, CA 94035–1000, and Search for Extraterrestrial Intelligence Institute, 2035 Landings Drive, Mountain View, CA 94043, USA.

*To whom correspondence should be addressed.

moving in the electric field of the free protons. The fluxes in the lines formed in this way are predicted to decrease with increasing n according to a power law whose index varies from approximately -6 to -7 at the smallest n to approximately -8 at $n \approx 40$ (17). Figure 2 compares the observed fluxes with the simplest spontaneous emission model—a power law with a constant “intermediate” value of the power index of -7 . The residual deviations from the model are remarkably small for two groups of lines: the optical-near-infrared lines [including the recently detected $H7\alpha$ at $19 \mu\text{m}$ (21)] and the radio lines. These lines embrace, in total, almost 5 decades in wavelength and almost 12 decades in intensity. This convincingly demonstrates that all these lines (except, perhaps, $H41\alpha$) are due to spontaneous emission. In contrast, the millimeter and submillimeter lines form a prominent “hump” above the interpolated level of spontaneous emission, which confirms that they are amplified by masing.

The newly detected infrared lines also show excess radiation above the predicted spontaneous level. $H10\alpha$ and $H12\alpha$ were measured 14 months apart, and the non-monotonic behavior of their excesses may result from variability that is similar to that observed for the masers in this source (14, 22). For both lines, the excess is smaller than for $H15\alpha$, which corroborates the suggestion (20) that observable lasing in MWC 349A vanishes somewhere near $n \approx 10$. We emphasize that the qualitative conclusion about a strong (more than an order of magnitude) excess in $H15\alpha$ does not change with the slight variations of the model power index [several models were tried; see, for example, (17)]. This result is based on the collective properties of a large number of lines, whence its robustness.

The detection of lasing in these lines proves that population inversions persist in the ionized recombining hydrogen down to at least $n \approx 10$ to 15, at densities as high as $\approx 10^5 \text{ cm}^{-3}$. This is in accordance with the population calculations (23) and demonstrates a basic understanding of the numerous fundamental quantum-mechanical processes controlling hydrogen populations at high densities.

It is easy to explain why detectable amplification turns on near $n \approx 40$. Past observations have revealed two morphological components in the envelope of MWC 349A: (i) an ionized outflow at $\approx 50 \text{ km s}^{-1}$ (24) and (ii) a circumstellar gas-dust disk (Fig. 3). Each line has an optimum gas density at which its amplification per unit length is maximum; the lower the n , the higher the optimum density. Recalling that

the density in the disk is proportional to $R^{-3/2}$, where R is the distance from the center, the lower the n of an α line, the smaller should be its masing (or lasing) ring. Calculations show (17) that gains are less than unity for the lines arising from $n \geq 40$, in the peripheral part of the disk, and explain why only spontaneous emission is observed. For $n \approx 36$ to 40, the gain along the ring chords first surpasses unity and then

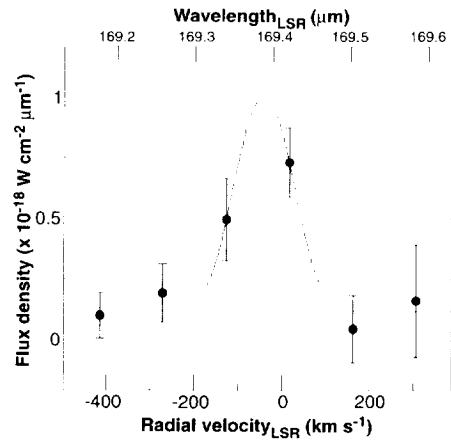


Fig. 1. The $H15\alpha$ spectral flux densities obtained from the KAO and the best fitted Gaussian line profile. LSR is the local standard of rest (for the stellar neighborhood of the sun).

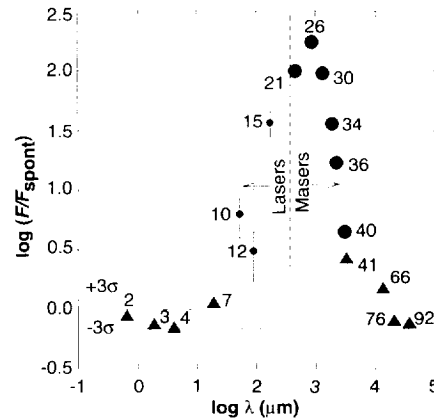


Fig. 2. A log-log plot of the ratio F/F_{spont} versus λ , where F is the observed integrated flux for an α line of wavelength λ , and $F_{\text{spont}} = -7 \times \log n - 12.24$. F_{spont} is a least squares fit to the optical-near-infrared and radio lines that estimates the contribution due to spontaneous emission. Triangles indicate spontaneous lines, large circles indicate masing millimeter and submillimeter lines, and small circles with error bars indicate our three KAO infrared detections. The dashed lines show $\pm 3\sigma$ from the fitted curve. The number near each symbol is the principal quantum number for that line’s lower level. The observed fluxes in the optical and near-infrared were corrected for extinction by circumstellar and interstellar dust (30). The largest measured fluxes (2, 14, 15) are plotted for the millimeter and submillimeter lines, which are known to be quite variable.

rises toward smaller n . This occurs even though the ring radius is decreasing—because of the strong dependence of the gain

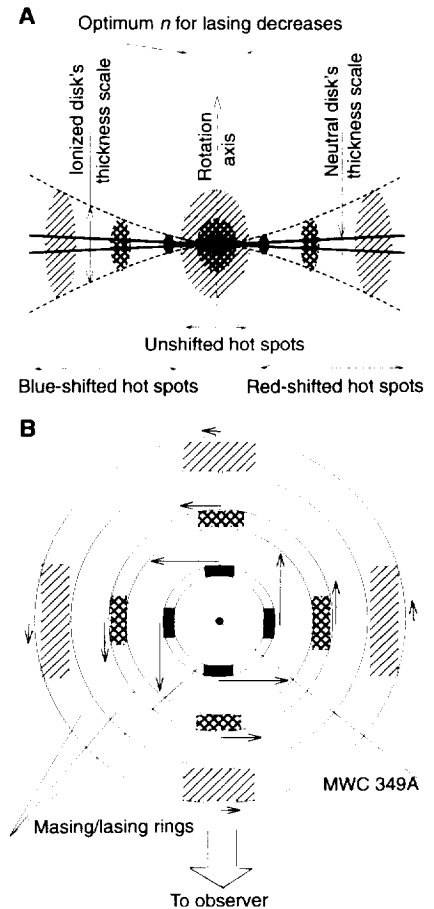


Fig. 3. The putative masing and lasing circumstellar disk in MWC 349A shown (A) edge-on (presumably as we observe it) and (B) face-on. The double-peaked profiles of some infrared and submillimeter spectral lines and the masing millimeter and submillimeter hydrogen lines are ascribed to a Keplerian circumstellar disk seen edge-on (14, 31). According to the model (32) we adopt here, the surface layer of the gas-dust disk surrounding MWC 349A is ionized by the star’s ultraviolet radiation and develops a hydrostatic 10^4 K atmosphere inside a critical distance $R_{\text{c}} \approx 200 \text{ AU}$. Because of decreasing gravitational binding, the atmosphere flares with distance from the star, and beyond R_{c} it transforms into a stationary bipolar outflow (the outflow is not shown). The electron density in the model atmosphere is $\approx 4 \times 10^5 \text{ cm}^{-3}$ at R_{c} and is proportional to $R^{-3/2}$ at smaller radii. The velocity vectors in (B) give a rough idea of the Keplerian rotation in the disk. The sense of the rotation is still unknown; it is shown arbitrarily here. The flaring of the disk and the positions and widths of the amplifying rings are not to scale (33). The shaded areas demonstrate the paths of maximal amplification in (B) and the resulting hot spots of maser and laser emission in (A). The increasing density of the shading (from diagonal through hatched to solid) toward the disk’s center illustrates the increasing gas density and, presumably, also the increasing brightness temperature of the masing and lasing hot spots.

on density—and gives rise to the strongly amplified lines making the hump shown in Fig. 2.

The more intriguing question is why does lasing apparently vanish at $n \approx 10$? At the moment, there are three possible explanations. (i) There is the possibility (15) that the disk only extends down to $R \approx 40$ astronomical units (AU), where its ionized density is $\sim 10^7$ to 10^8 cm^{-3} , which is the optimum for amplification of the lines with $n \approx 20$. Because the lines with lower n require progressively higher densities, the intensity generated in this innermost ring decreases with decreasing n . It is estimated (20) that in this case lasing becomes undetectable near $n \approx 10$. (ii) If we assume that the disk continues inward of ≈ 40 AU and that each lasing line forms at its optimum density, then it can be shown (17) that for $n \leq 30$ the amplification “saturates,” which slows the increase of intensity with decreasing n . Furthermore, the size of the lasing hot spot decreases with decreasing n (Fig. 3), so that the flux due to spontaneous emission, which arises from the source as a whole, becomes increasingly dominant, and at $n \approx 10$ the lasing component becomes undetectable on this bright spontaneous background. If this is the case, future infrared interferometers will detect small (0.1 to 0.01 arc sec) bright hot spots lasing in the near-infrared hydrogen α lines in the inner disk. (iii) It is also predicted in the latter model that the laser solid angle Ω increases with n as $\Omega \propto n^{1/2}$. If the disk is tilted slightly from our line of sight, this would remove the low- n lasers from our view first. Future observations should help choose between these (and perhaps other) possibilities. Hypothesis (ii)—the competition between the laser and the spontaneous emission—may provide a clue for understanding the general lack of observed astrophysical lasers.

The brightness temperature (T_B) and amplification of these lasers can be calculated once their angular sizes are known. To get a rough estimate, we assume that the disk continues inward of ≈ 40 AU and that H15 α forms in the disk at its optimum density of $N_e \approx 1 \times 10^9 \text{ cm}^{-3}$, which occurs in the model at a radial distance $r \approx 5$ AU from the star (17). We also assume that H15 α is a single-peaked line—any narrow double-peaked component will have an even higher brightness temperature. Taking r as an upper limit to the linear scale of the laser's hot spot and assuming a line width $\Delta v \approx 70 \text{ km s}^{-1}$ (2), we obtain $T_B \approx (\lambda^3 F D^2)/(2k \Delta v r^2) \sim 10^7 \text{ K}$, where λ is the wavelength, k is Boltzmann's constant, F is the observed integrated flux, and D is the distance to the star [$\approx 1200 \text{ pc}$ (10)]. If the

input radiation temperature of the laser is equal to the typical physical temperature of the gas in an HII region ($\sim 10^4 \text{ K}$), then the amplification factor is $A \approx 10^3$. Similar values of T_B and A are estimated for the H10 α line. Thus, these far-infrared lasers may be rather strong amplifiers, with amplification factors and brightness temperatures comparable to or greater than those for the millimeter masers in this source (22). Whereas the amplification in hydrogen is expected to limit gains and brightness temperatures to less dramatic values than those for the strongest molecular masers (17), the estimated luminosities in the lasing hydrogen lines, ~ 0.01 to $0.1 L_\odot$, are comparable to those of the strongest galactic molecular masers (25).

Detection of these new lines was due to their lasing, because purely spontaneous lines would be below our KAO detection thresholds. Observations with higher signal-to-noise ratios and improved spectral resolution ($\leq 10 \text{ km s}^{-1}$) are still desirable. The Infrared Satellite Observatory will hopefully provide higher signal-to-noise flux measurements for all the lines in the far infrared. The Stratospheric Observatory for Infrared Astronomy (26) will have sufficient spectral resolution to observe any double-peaked velocity structure, enabling us to precisely locate the lasers in the Keplerian disk and thereby ascertain whether the disk has a void inward of $R \approx 40$ AU, which is important for understanding planet formation in such disks (27).

REFERENCES AND NOTES

1. H. Weaver, D. R. W. Williams, N. H. Dieter, W. T. Lum, *Nature* **208**, 29 (1965); A. C. Cheung, D. M. Rank, C. H. Townes, D. D. Thornton, W. J. Welch, *ibid.* **221**, 626 (1969).
2. C. Thum *et al.*, *Astron. Astrophys.* **288**, L25 (1994).
3. K. M. Menten and K. Young, *Astrophys. J.* **450**, L67 (1995).
4. *Encyclopaedia Americana*, 1984 ed., Masers; *ibid.*, Lasers; K.-J. Kim and A. Sessler, *Science* **250**, 88 (1990).
5. M. J. Seaton, *Mon. Not. R. Astron. Soc.* **119**, 90 (1959).
6. J. H. Krolik and C. F. McKee, *Astrophys. J. Suppl. Ser.* **37**, 459 (1978).
7. H. A. Smith, H. P. Larson, U. Fink, *Astrophys. J.* **233**, 132 (1979).
8. N. Scoville, S. Kleinmann, D. Hall, S. Ridgway, *ibid.* **275**, 201 (1984).
9. M. J. Mumma *et al.*, *Science* **212**, 45 (1981); B. F. Gordiets and V. Ya. Panchenko, *Cosmic Res. USA* **21**, 725 (1983); G. I. Stepanova and G. M. Shved, *Sov. Astron. Lett.* **11**, 390 (1985); R. E. Dickinson and S. W. J. Bougher, *Geophys. Res.* **91**, 70 (1986); M. Mumma, in *Astrophysical Masers*, A. W. Clegg and G. E. Nedoluha, Eds. (Springer-Verlag, Berlin, 1993), p. 455.
10. M. Cohen, J. H. Bieging, J. W. Dreher, W. J. Welch, *Astrophys. J.* **292**, 249 (1985).
11. P. W. Merrill and C. G. Burwell, *ibid.* **78**, 87 (1933).
12. L. F. Rodriguez and T. S. Bastian, *ibid.* **428**, 324 (1994).
13. J. Martin Pintado, R. Bachiller, C. Thum, C. M. Walmsley, *Astron. Astrophys.* **215**, L13 (1989).

14. C. Thum, J. Martin-Pintado, R. Bachiller, *ibid.* **256**, 507 (1992).
15. C. Thum *et al.*, *ibid.* **283**, 582 (1994).
16. C. Thum, V. S. Strelitski, J. Martin-Pintado, H. E. Matthews, H. A. Smith, *ibid.* **300**, 843 (1995).
17. V. S. Strelitski, V. O. Ponomarev, H. A. Smith, *Astrophys. J.*, in press; V. S. Strelitski, H. A. Smith, V. O. Ponomarev, *ibid.*; H. A. Smith, V. S. Strelitski, V. O. Ponomarev, in *Amazing Light*, R. Y. Chiao, Ed. (Springer-Verlag, New York, 1996), p. 603.
18. E. F. Erickson *et al.*, *Proc. Soc. Photo-Opt. Instrum. Eng.* **509**, 129 (1984).
19. These transitions were chosen because they are relatively free of telluric absorption at KAO altitudes. The H10 α and H12 α lines and adjacent continua were observed with 11 Ge:Sn photoconductors, and the H15 α line and continuum were observed with six stressed Ge:Ga photoconductors. Standard chopping and nodding techniques (28) were used throughout. The raw spectra were flat-fielded with the use of Saturn observations at the same wavelengths on the same flights. The absolute flux calibration was accomplished by multiplication of these ratioed spectra by the flux of Saturn as computed from the disk and ring contributions, with the use of a geometric model of the system (29). The total integration times for the three lines were 5200, 7440, and 4240 s. The quoted errors of our measurements are statistical only and represent one standard deviation from the mean. The calibration uncertainty of $\pm 25\%$ does not substantially increase the total uncertainty.
20. V. S. Strelitski *et al.*, in *Proceedings of the Airborne Astronomy Symposium on the Galactic Ecosystem: From Gas to Stars to Dust*, NASA, NASA Ames Research Center, 5 to 8 July 1994, M. R. Haas, J. A. Davidson, E. F. Erickson, Eds. (Astronomical Society of the Pacific, San Francisco, CA, 1995), p. 271.
21. H. A. Smith *et al.*, in preparation.
22. J. Martin-Pintado, C. Thum, R. Bachiller, *Astron. Astrophys.* **229**, L9 (1989).
23. P. J. Storey and D. G. Hummer, *Mon. Not. R. Astron. Soc.* **272**, 41 (1995).
24. W. J. Altenhoff, P. A. Strittmatter, H. J. Wendker, *Astron. Astrophys.* **93**, 48 (1981).
25. C. R. Gwinn, J. M. Moran, M. J. Reid, *Astrophys. J.* **393**, 149 (1992).
26. E. F. Erickson and J. A. Davidson, in *Proceedings of the Airborne Astronomy Symposium on the Galactic Ecosystem: From Gas to Stars to Dust*, M. R. Haas, J. A. Davidson, E. F. Erickson, Eds. (Astronomical Society of the Pacific, San Francisco, CA, 1995), p. 707.
27. F. H. Shu, D. Johnston, D. Hollenbach, *Icarus* **106**, 92 (1993).
28. R. Popovular, *Astron. Astrophys.* **117**, 46 (1983).
29. B. Bezard, D. Gautier, A. Marten, *ibid.* **161**, 387 (1986); M. R. Haas, E. F. Erickson, D. D. McKibbin, D. Goorvitch, L. J. Caroff, *Icarus* **51**, 476 (1982); S. Matthews and E. F. Erickson, NASA Technical Memorandum X-73204, p. 1 (1977).
30. R. I. Thompson, P. A. Strittmatter, E. F. Erickson, F. L. Witteborn, D. W. Strecker, *Astrophys. J.* **218**, 170 (1977).
31. F. Hamann and M. Simon, *ibid.* **311**, 909 (1986); M. A. Gordon, *ibid.* **387**, 701 (1992).
32. D. Hollenbach, D. Johnstone, S. Lizano, F. Shu, *ibid.* **428**, 654 (1994).
33. Laser amplification requires velocity coherence along the line of sight. In a narrow Keplerian ring seen edge-on, the coherent path is maximum along the two longest line-of-sight chords. Because of rotation, the chords produce two spectral components that are red-shifted and blue-shifted, respectively, relative to the central star. If the ring is wide, the gain along the central diameter can also be sufficient to produce an amplified component at zero Doppler-shift.
34. We gratefully acknowledge the KAO staff for their support of our expedition to Hawaii, J. Baltz for his laboratory and flight support, and R. Squire for useful comments and for suggesting the format of Fig. 3. Supported by NASA and the Smithsonian Institution.

28 February 1996; accepted 18 April 1996